Applied Physics Letters

Single-electron pump with highly controllable plateaus

Cite as: Appl. Phys. Lett. **119**, 153102 (2021); https://doi.org/10.1063/5.0067428
Submitted: 16 August 2021 • Accepted: 22 September 2021 • Published Online: 11 October 2021

H. Howe, M. Blumenthal, H. E. Beere, et al.

Applied Physics Letters ARTICLE scitation.org/journal/apl

Single-electron pump with highly controllable plateaus

Cite as: Appl. Phys. Lett. **119**, 153102 (2021); doi: 10.1063/5.0067428
Submitted: 16 August 2021 · Accepted: 22 September 2021 ·
Published Online: 11 October 2021

View Online Export Citation CrossMark

H. Howe,[1,a)] M. Blumenthal,[2] H. E. Beere,[3] T. Mitchell,[3] D. A. Ritchie,[3] and M. Pepper[1]

AFFILIATIONS

[1]University College London, London Centre for Nanotechnology and Department of EE, London WC1A 0AH, United Kingdom
[2]Physics Department, University of Cape Town, Rondebosch 7700, South Africa
[3]Physics Department, Cavendish Laboratory, University of Cambridge, Cambridge CB3 0HE, United Kingdom

[a)]Author to whom correspondence should be addressed: uceehhh@ucl.ac.uk

ABSTRACT

Future quantum based electronic systems will demand robust and highly accurate on-demand sources of current. The ultimate limit of quantized current sources is a highly controllable device that manipulates individual electrons. We present a GaAs single-electron pump, where electrons are pumped through a one-dimensional split-gate saddle point confinement potential, which show quantized plateaus with length and width that can be independently tuned with the application of a source-drain bias and RF amplitude. The plateaus can be over two orders of magnitude longer than conventional pumps, and flatness improves with the application of a source-drain bias.

Single-electron pumps allow for the on-demand supply of electrons with a high degree of precision. The pumps are promising building-blocks for solid-state quantum computation based on electron-quantum-optic devices,[1–3] where the pump is used as a controllable electron source incident on electrostatic barriers. They are also a leading contender for the calibration of the SI unit, Ampère, based on its redefinition in terms of the fundamental charge of the electron, *e*.[4]

Initially, electron-counting devices were based on resonant tunneling through a quantum dot (QD).[5–7] Later, surface acoustic waves on gallium arsenide (GaAs) were used to move single electrons over a barrier.[8,9] To pump at higher frequencies, non-adiabatic dynamic QD pumps were developed, which operated like a quantum charged coupled device (CCD).[10] An oscillating voltage is applied to a gate such that the QD forms, trapping electrons at the Fermi level and pushing them over a barrier each cycle. A simple two gated CCD has widely been adopted as the mechanism for producing high-accuracy single-electron current.[11,12] Further improvements have been found at lower temperatures and in high magnetic fields[13] and are also being studied in silicon.[14,15] Comprehensive reviews are given by Giblin *et al.* and Bäuerle *et al.*[16,17] with errors associated with back-tunneling discussed by Kashcheyevs and Kaestner.[18,19]

In this Letter, we present a pump that has a split-gate with a saddle point potential as the exit gate, rather than a more conventional finger gate. In the absence of a magnetic field, we can induce quantized current in such pumps by increasing the source-drain bias voltage. The induced current is extremely stable with respect to the exit gate voltage. With the plateau length defined in terms of fitting parameters to the universal decay cascade model (UDC),[18,19] the plateaus can be over two orders of magnitude longer than those of conventional pumps and turnstiles. Control of the source-drain bias (V_{bias}) and RF amplitude (A_{RF}) allows for the plateau's length, width, and minimum slope to be tuned independently. This will enable experimenters that would otherwise not be able to see pumping in their preferred parameter space to tune into a quantized pumping regime by changing one of these additional parameters. Additionally, the independent tuning may lead to a better understanding of the physical mechanism and improved modeling of the full design range of single-electron pumps.

The measurement circuit and device are shown in Fig. 1. The device was fabricated on MBE grown high mobility GaAs/$Al_xGa_{1-x}As$ Si-doped 2DEG wafers with the 2DEG 90 nm below the surface (10 nm GaAs cap, 40 nm Si-doped GaAs/$Al_xGa_{1-x}As$, 40 nm GaAs/$Al_xGa_{1-x}As$ spacer, and GaAs substrate)carrier density $n = 1.9 \times 10^{11}$ cm^{-2}, mobility $\mu = 1.014 \times 10^6$ cm^2/V s). The 2DEG channel pattern was defined using electron-beam lithography (EBL) and etched to a depth of 40 nm using wet chemistry. The gates were defined using EBL and deposited with 120 nm of Ti/Au in a thermal evaporator. The devices were loaded into a dilution fridge with a base temperature of 7 mk. Outside the fridge, current was measured using a

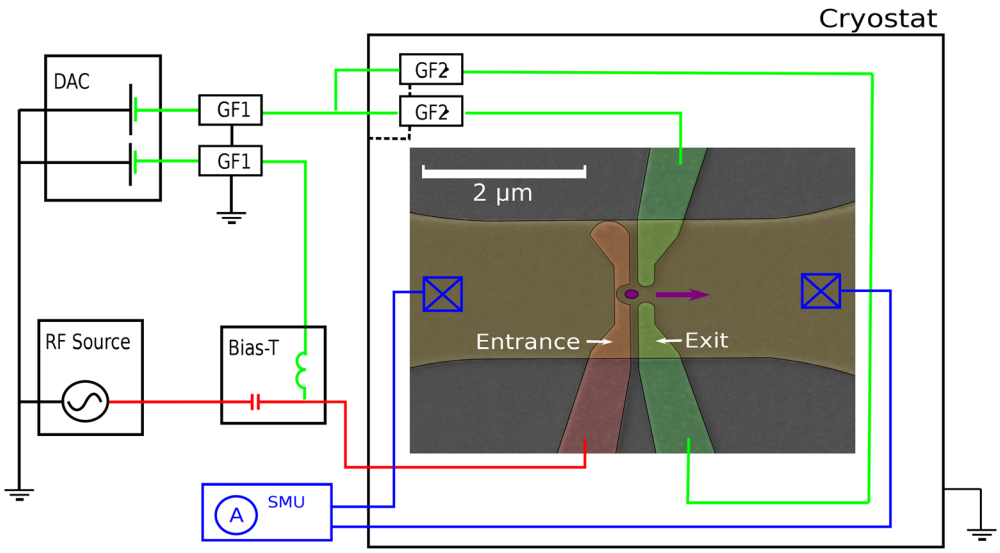

FIG. 1. Schematic of the experimental setup showing external equipment and connections to the device in the dilution fridge. A digital to analogue converter (DAC) supplies a DC voltage through gate filters (GF1 and GF2), and an RF source supplies an oscillating voltage via a coaxial line (red). A false-color scanning electron microscope (SEM) image of the device shows a 2 μm wide 2DEG channel (yellow), formed by etching away the substrate around the channel, and the Ti/Au entrance and exit gates (red and green). When voltages are applied to the gates, they form an electrostatic QD (purple). The RF voltage added to the entrance gate pumps electrons to the right.

Keithley 6430 source measure unit (SMU), which was connected to the drain side of the pump. A NI2969 cDAQ provided the voltages that were applied to the gates. The RF source was a HP E4400B. The effects have been observed in two devices with similar device structure and fabrication but only data from one device are presented to focus on the parameter dependence of the device. More details of the setup are given in the supplementary material.

Measuring current vs V_{Exit} and V_{Ent}, we create a 2D color-map "pumpmap" from which we investigate the effects of the control parameters. All data are taken at T = 45 mK with no magnetic field (B = 0 T) and frequency = 180 MHz, except where stated otherwise. Data in Fig. 2 have $A_{RF} = 220$ mV. Figure 2(a) shows derivative pumpmaps, dI/dV_{Exit}, at different V_{bias}. The plateaus are enclosed by onset, ejection, and capture lines, all of which mark the transition from no pumped current to quantized pumping. In the thermal regime, the first onset line marks the transition where a QD, of size determined by the gate voltages intersecting the onset line, forms at the Fermi level. The ejection lines mark where V_{Ent} is negative enough to push the electron over the split-gate potential. Only the ejection line that corresponds to the first plateau in each pumpmap is shown. Apart from a small slope, likely due to cross-talk between the gates, the ejection lines are independent of $V_{Exit.}$ The capture line marks where V_{Ent} is set such that the dot forms at the Fermi level. The first plateau has a plateau width (purple arrow) between the capture and ejection lines and a plateau length (red arrow) between the onset lines of the first and second plateaus.

At $V_{bias} = 60$ mV, the plateau length is ≈0.11 V. As the pump is forward biased (V_{bias} is made more positive), the onset lines become more curved and the plateaus lengthen, while the plateau widths remain fixed. The pumpmap at $V_{bias} = 120$ mV shows a markedly increased plateau length of ≈0.60 V.

This new dependence on V_{bias} makes it the only *in situ* parameter for controlling the length of a plateau at fixed V_{Ent}, other than applying a high magnetic field. The physical mechanisms that govern the changes in the pumpmaps due to the changes in applied gate voltages, source-drain bias, RF amplitude, and magnetic fields are still not well understood in the community, but the empirical improvement observed when applying a high magnetic field makes it the standard operating regime for metrological studies. In split-gate pumps, the empirical improvement with V_{bias} can hopefully be utilized as well.

Figure 2(b) shows the minimum slope of the first plateau from the pumpmaps at different V_{bias}. To look at the flatness in low resolution data, usually a "fingerprint" of flatness is used, based on fits to the UDC model. This method is not applicable to our data as it assumes the curvature parameter in the fit to be the same for different plateaus. Instead, we measured the slope directly by applying a numerical derivative to the data. As V_{bias} increases, the minimum slope decreases from 6.1×10^{-4} ef/mV at $V_{bias} = -65$ mV to 3.3×10^{-5} ef/mV at $V_{bias} = 95$ mV. Beyond this, the slope becomes comparable to the noise of the data acquisition setup, and we cannot easily resolve a slope. Measurement for metrology needs to be done empirically, as fits do not necessarily capture all the error mechanisms in the pumping process, and currently, there is no theoretical framework that describes all the error mechanisms and provides a good fit to the data. Many pumps at these low frequencies are already ideally flat to within the measurement capabilities of metrology laboratories but only in a large magnetic field. At the higher frequencies that are of interest to metrology, the slope becomes less flat. Our split-gate pumps show that flatness can be improved by applying a source-drain bias.

Figure 2(c) shows a derivative pumpmap, dI/dV_{Exit} against V_{Exit} and $V_{bias.}$ When V_{bias} is increased, the plateaus shift to more negative V_{Exit} and the plateau length increases sharply. This means that at a given V_{Exit}, quantized pumping can be induced by increasing V_{bias}, and very long quantized plateaus can be generated. The long plateaus offer the experimenter fine control of ejection energies, as they only

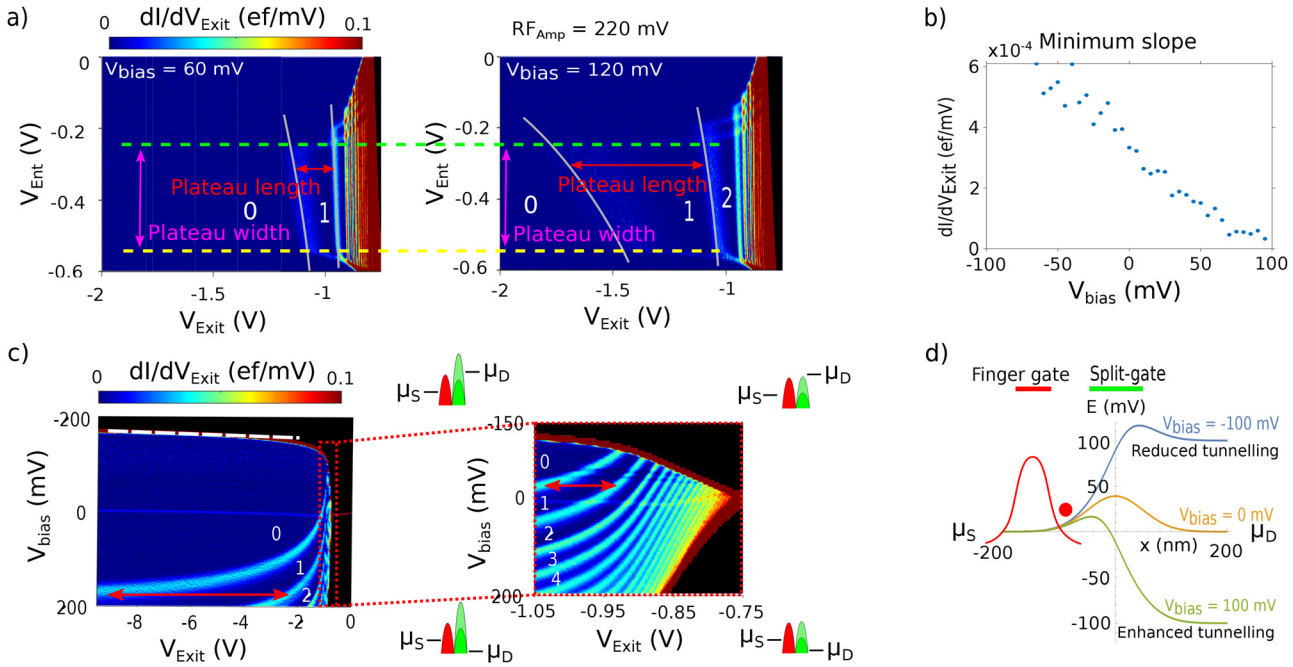

FIG. 2. (a) Pumpmaps, dI/dV_{Exit}, at different source-drain voltage biases. The dark blue regions show where there is no change in current. The number of pumped electrons per cycle is shown in white. The first plateau is bordered by onset lines (gray) either side, a capture line (dashed yellow) below, and an ejection line (dashed green) above. The black region is where the electrometer is out of range as Ohmic current dominates the pumped current. As V_{bias} is increased, the plateau length increases but the plateau width remains constant. (b) Minimum slopes, dI/dV_{Exit}, of the linescans at $V_{Ent} = -0.3$ V for different V_{bias}. (c) Plot of dI/dV_{Exit} vs V_{bias} and V_{Exit} at $V_{Ent} = -0.3$ V. The dashed white line is used for the lever arm term calculation. The lighter blue vertical line near $V_{bias} = 0$ mV appears to be a measurement artifact. The region near the gate pinch-off (red rectangle) is shown in higher resolution on the right. Schematics in the corners are a guide showing the relative entrance and exit gate potentials (red and green) of a cross section of a split-gate pump. (d) Electrostatic potential model of the source drain bias effect on split-gate potential.

change slightly with voltage applied to the exit split-gate. The potential energy at the 2DEG due to the exit gate voltage can be approximated from the contour line where the Ohmic current starts. The lever arm, α, which maps the applied gate voltage to a potential energy by $E = \alpha \times V + \text{offset}$, is not constant in our device. As V_{bias} becomes more negative, α becomes very small [slope of the dashed white line in Fig. 2(b)].

Pumping with $V_{Exit} = -4$ V would have a corresponding peak barrier energy of 160 meV [on the white dashed line in Fig. 2(b)]. The energy of the pumped electrons is assumed to be near the peak energy of the barrier.[1] The 160 meV is comparable to the measured ejection energy in the literature of $\geq$150 meV[1] for a finger gate pump at $V_{Exit} \approx -0.5$ V with $V_{bias} \leq 10$ mV. Our pump requires a much larger V_{bias} than what is usually applied to the finger gate pump, but the energies appear to be stable in V_{exit} once V_{bias} is large enough. There is a difficulty in using V_{bias} to calibrate the energy of a gate defined potential when the gate potential is dependent on V_{bias}, and ideally a device with a second barrier could be used to measure the ejection energies directly.

In finding a physical mechanism for the source-drain dependence, we examine previous literature on QPC gate potentials under source-drain bias, which shows that the bias has a direct influence on the effective gate potentials and tunnel current.[20,21] We invoke a model detailed by Gloos *et al.*,[22] where a hard-wall potential with eigen energies given by

$$E_n[w(x)] = \frac{n^2 h^2}{8 m^* w^2(x)}, \tag{1}$$

is used instead of a more conventional saddle-point approximation. Here, h is Planck's constant, $m^* = 0.067 m_e$ is the effective electron mass in GaAs, the index n denotes the different 1D subbands, and $w(x)$ is the width of the constriction approximated by an inverted Gaussian given by

$$w(x) = w_0 \exp\left(\frac{x^2}{L^2}\right). \tag{2}$$

Here, w_0 is the minimum width of the unbiased constriction at a fixed gate voltage and L defines its length. In the far pinched-off regime, the applied source-drain bias changes the barrier energy as seen by the electrons in the 2DEG. This change in electrostatic energy is approximated by

$$E_{bias}(x) \approx -\frac{eV_{bias}}{2}\left[1 + \tanh\left(\frac{5x}{2L}\right)\right], \tag{3}$$

which is added to the eigen energies given in Eq. (1).

Figure 2(d) shows the variation of the potential energy of the QPC with $V_{bias} = -100$ mV (blue), 0 mV (yellow), and 100 mV (green). As the potential of the drain is lowered, the effective exit barrier height is also lowered and the dot gets bigger. This induces pumped current where otherwise the dot would be too small and allows for pumping over a larger range of gate voltages. Gloos *et al.*[22] indicate that this regime of transport is due to quantum tunneling

through the saddle-point potential and not thermal effects due to local heating from the applied source-drain.

Figure 3(a) shows pumpmaps at different RF amplitudes with fixed $V_{bias} = 60$ mV. At $A_{RF} = 200$ mV, the plateau length is 420 mV. As A_{RF} is increased, the position of the onset lines is unchanged, and the plateau length at a given V_{Ent} remains constant. However, as the first and second onset lines have different curvatures, we can measure longer plateau lengths at less negative V_{Ent}. As A_{RF} increases, the plateau width increases linearly, pushing out the capture and ejection lines equally. Plateau width $= 3.5 \times (A_{RF} - 125\,\text{mV})$. Although the plateau width is larger than the applied RF amplitude, this is attributed to the cross coupling of the gates. This linear dependence agrees with the literature on conventional pumps.[23] We do not observe a reduction in the minimum slope as we did for increased V_{bias}, as the onset lines do not move.

Figure 3(b) shows line scans at different V_{bias} with $A_{RF} = 400$ mV and $V_{Ent} = -0.3$ V. Our investigation was restricted to a maximum voltage applied to the split gate of −9.5 V, but currently no upper limited has been determined for the length of plateau as a function of the split-gate voltage. The plateau length in Fig. 3(b) as defined from the UDC fit is 10.26 V. Note that while the plateau extends beyond the left of the plot, we can still use the fit from a partial section of the plateau to determine its length. To do this, we fit the UDC double exponential fitting equation

$$I = (ef)\sum_{n} \exp\left[-\exp\left(-\alpha_n(V_{Exit} + \delta_n)\right)\right], \tag{4}$$

and extract the length.[18] Here, α_n and δ_n are fitting parameters over n plateaus. α_n (different to the lever term α discussed earlier) gives the curvature of the rise from the n–1-th to the n-th plateau with a large α_n being more step-function-like. δ_n are locations in V_{Exit} of the transition between plateaus $n - 1$ and n. The plateau length can be defined as $L_{plateu-n} = \delta_{n+1} - \delta_n$. Note that our use of α_n and δ_n differ slightly from the parameters α and Δ used in the UDC model.

In our split-gate pumps, a change in A_{RF} results in a change in the plateau width without modifying the plateau length at a fixed V_{Ent}. A change in V_{bias} results in a change in the plateau length without modifying the plateau width. Combining these two effects allows for a level of control not seen before in conventional pumps. Figure 3(c) is a derivative pumpmap, dI/dV_{bias} vs V_{bias} and A_{RF}, at fixed $V_{Ent} = -0.3$ V and $V_{Exit} = -1.2$ V. The pumpmap shows an unexpected structure at the boundary of non-pumping to pumping (red dashed line). This structure is similar in shape to the boundary of non-pumping to pumping in the ejection lines of a standard V_{Exit} and V_{Ent} pumpmap,[10] suggesting that the V_{bias} and A_{RF} have a similar effect on the size of the QD at key points in the pumping cycle. The effect that V_{bias} and A_{RF} have on the potentials at the exit and entrance gates may be equivalent to manipulating V_{Exit} and V_{Ent} directly. The lighter blue vertical line near $V_{bias} = 0$ mV is a measurement artifact.

A simple design change to the gates defining the dynamic QD allows single-electron pumps to be tuned by a source-drain bias. This source-drain bias dependence, together with the RF amplitude dependence, gives researchers in the fields of quantum information and metrology two experimental parameters for maximizing the robustness of single electron pumping in both gate voltages defining the QD. The design changes are unobtrusive and still allow for the ability to integrate our device into more complicated quantum based electronic

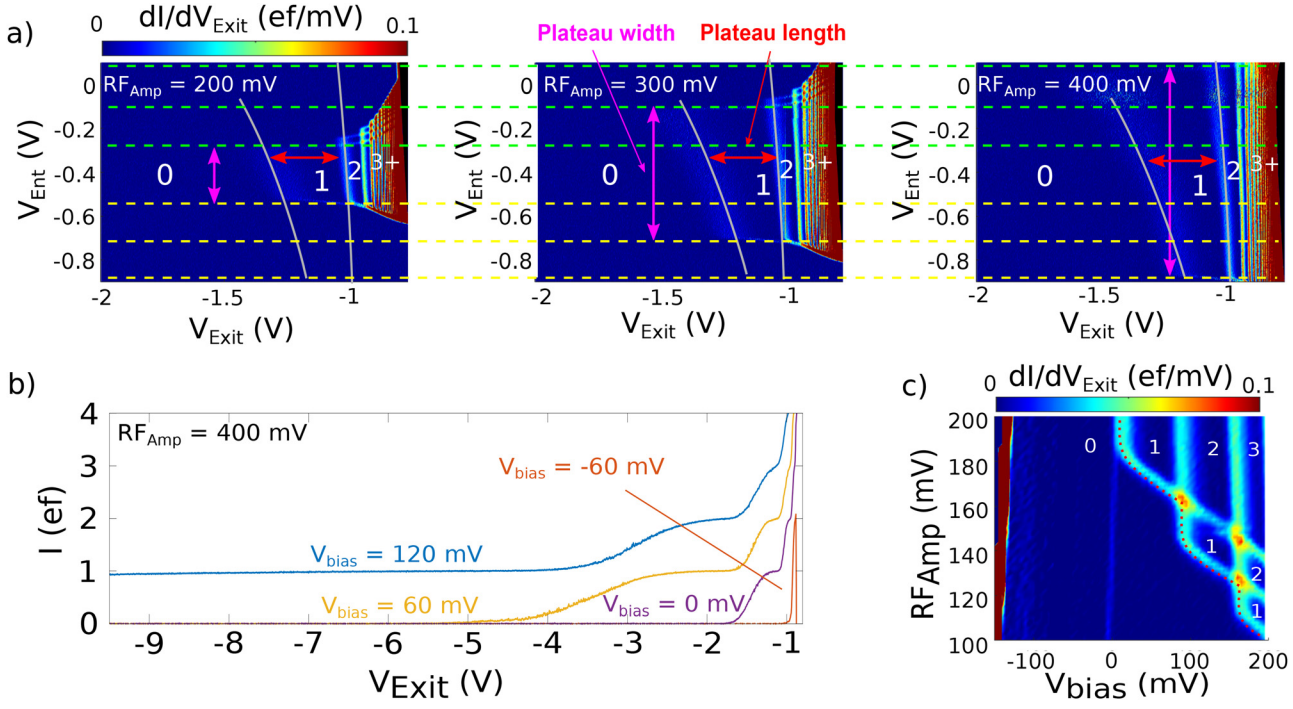

FIG. 3. (a) Pumpmaps dI/dV_{Exit} at different RF amplitudes. (b) Pump plateaus at different V_{bias} with $A_{RF} = 400$ mV and $V_{Ent} = -0.3$ V. (c) Derivative plot of current against V_{bias} and RF amplitude.

systems and more sophisticated high-accuracy measurement setups. Initial results indicate a substantial improvement in the minimum slope when increasing V_{bias}, which is measured on a standard non-metrological grade measuring system. To improve in accuracy, these pumps could be measured by metrological institutes incorporating years of advancements in measuring techniques, coupled with highly calibrated traceable instruments.[24] By offering an additional control parameter via the source-drain bias, these pumps can be tuned into the desired quantized pumping level in the far pinched-off regime that has been until now, previously inaccessible with conventional pumps.

See the supplementary material for details of the experimental setup, plateau fitting, and lever arm term.

This work was supported by the UK Engineering Physical Sciences Research Council, Grant Nos. EP/K004077/1, EP/R029075/1, and EP/P021859/1 and the National Research Foundation of South Africa and Sasol. We would also like to acknowledge a fruit-full discussion with M. Kataoka, S. Giblin, and J. Fletcher at the National Physical Laboratory.

AUTHOR DECLARATIONS

Author Contributions

H.H. and M.B. contributed equally to this work.

DATA AVAILABILITY

The data that support the findings of this study are available from the corresponding author upon reasonable request.

REFERENCES

[1]J. D. Fletcher, P. See, H. Howe, M. Pepper, S. P. Giblin, J. P. Griffiths, G. A. C. Jones, I. Farrer, D. A. Ritchie, T. J. B. M. Janssen, and M. Kataoka, "Clock-controlled emission of single-electron wave packets in a solid-state circuit," Phys. Rev. Lett. **111**, 216807 (2013).
[2]N. Johnson, J. D. Fletcher, D. A. Humphreys, P. See, J. P. Griffiths, G. A. C. Jones, I. Farrer, D. A. Ritchie, M. Pepper, T. J. B. M. Janssen, and M. Kataoka, "Ultrafast voltage sampling using single-electron wavepackets," Appl. Phys. Lett. **110**, 102105 (2017).
[3]N. Ubbelohde, F. Hohls, V. Kashcheyevs, T. Wagner, L. Fricke, B. Kästner, K. Pierz, H. W. Schumacher, and R. J. Haug, "Partitioning of on-demand electron pairs," Nat. Nanotechnol. **10**, 46–49 (2015).
[4]S. P. Giblin, M. Kataoka, J. D. Fletcher, P. See, T. J. B. M. Janssen, J. P. Griffiths, G. A. C. Jones, I. Farrer, and D. A. Ritchie, "Towards a quantum representation of the ampere using single electron pumps," Nat. Commun. **3**, 930 (2012).
[5]P. Delsing, K. K. Likharev, L. S. Kuzmin, and T. Claeson, "Time-correlated single-electron tunneling in one-dimensional arrays of ultrasmall tunnel junctions," Phys. Rev. Lett. **63**, 1861–1864 (1989).
[6]L. P. Kouwenhoven, A. T. Johnson, N. C. van der Vaart, C. J. P. M. Harmans, and C. T. Foxon, "Quantized current in a quantum-dot turnstile using oscillating tunnel barriers," Phys. Rev. Lett. **67**, 1626–1629 (1991).
[7]M. W. Keller, J. M. Martinis, N. M. Zimmerman, and A. H. Steinbach, "Accuracy of electron counting using a 7-junction electron pump," Appl. Phys. Lett. **69**, 1804–1806 (1996).
[8]J. Cunningham, V. I. Talyanskii, J. M. Shilton, M. Pepper, A. Kristensen, and P. E. Lindelof, "Single-electron acoustic charge transport on shallow-etched channels in a perpendicular magnetic field," Phys. Rev. B **62**, 1564–1567 (2000).
[9]P. Delsing, A. Cleland, M. Schuetz, J. Knörzer, G. Giedke, J. Cirac, K. Srinivasan, M. Wu, K. Balram, C. Bäuerle, T. Meunier, C. Ford, P. Santos, E. Cerda-Méndez, H. Wang, H. Krenner, E. Nysten, M. Weiß, G. Nash, L. Thevenard, C. Gourdon, P. Rovillain, M. Marangolo, J.-Y. Duquesne, G. Fischerauer, W. Ruile, A. Reiner, B. Paschke, D. Denysenko, D. Volkmer, A. Wixforth, H. Bruus, M. Wiklund, J. Reboud, J. Cooper, Y. Fu, M. Brugger, F. Rehfeldt, and C. Westerhausen, "The 2019 surface acoustic waves roadmap," J. Phys. D: Appl. Phys. **52**, 353001 (2019).
[10]M. D. Blumenthal, B. Kaestner, L. Li, S. Giblin, T. J. B. M. Janssen, M. Pepper, D. Anderson, G. A. C. Jones, and D. A. Ritchie, "Gigahertz quantized charge pumping," Nat. Phys. **3**, 343–347 (2007).
[11]B. Kaestner, V. Kashcheyevs, S. Amakawa, M. Blumenthal, L. Li, T. Janssen, G. Hein, K. Pierz, T. Weimann, U. Siegner *et al.*, "Single-parameter nonadiabatic quantized charge pumping," Phys. Rev. B **77**, 153301 (2008).
[12]A. Fujiwara, K. Nishiguchi, and Y. Ono, "Nanoampere charge pump by single-electron ratchet using silicon nanowire metal-oxide-semiconductor field-effect transistor," Appl. Phys. Lett. **92**, 042102 (2008).
[13]S. J. Wright, M. D. Blumenthal, G. Gumbs, A. L. Thorn, M. Pepper, T. J. B. M. Janssen, S. N. Holmes, D. Anderson, G. A. C. Jones, C. A. Nicoll, and D. A. Ritchie, "Enhanced current quantization in high-frequency electron pumps in a perpendicular magnetic field," Phys. Rev. B **78**, 233311 (2008).
[14]A. Rossi, T. Tanttu, K. Y. Tan, I. Iisakka, R. Zhao, K. W. Chan, G. C. Tettamanzi, S. Rogge, A. S. Dzurak, and M. Möttönen, "An accurate single-electron pump based on a highly tunable silicon quantum dot," Nano Lett. **14**, 3405–3411 (2014).
[15]A. Rossi, J. Klochan, J. Timoshenko, F. E. Hudson, M. Möttönen, S. Rogge, A. S. Dzurak, V. Kashcheyevs, and G. C. Tettamanzi, "Gigahertz single-electron pumping mediated by parasitic states," Nano Lett. **18**, 4141–4147 (2018).
[16]S. P. Giblin, A. Fujiwara, G. Yamahata, M.-H. Bae, N. Kim, A. Rossi, M. Möttönen, and M. Kataoka, "Evidence for universality of tunable-barrier electron pumps," Metrologia **56**, 044004 (2019).
[17]C. Bäuerle, D. C. Glattli, T. Meunier, F. Portier, P. Roche, P. Roulleau, S. Takada, and X. Waintal, "Coherent control of single electrons: A review of current progress," Rep. Prog. Phys. **81**, 056503 (2018).
[18]V. Kashcheyevs and B. Kaestner, "Universal decay cascade model for dynamic quantum dot initialization," Phys. Rev. Lett. **104**, 186805 (2010).
[19]V. Kashcheyevs and J. Timoshenko, "Quantum fluctuations and coherence in high-precision single-electron capture," Phys. Rev. Lett. **109**, 216801 (2012).
[20]L. P. Kouwenhoven, B. J. van Wees, C. J. P. M. Harmans, J. G. Williamson, H. van Houten, C. W. J. Beenakker, C. T. Foxon, and J. J. Harris, "Nonlinear conductance of quantum point contacts," Phys. Rev. B **39**, 8040–8043 (1989).
[21]N. K. Patel, L. Martin-Moreno, M. Pepper, R. Newbury, J. E. F. Frost, D. A. Ritchie, G. A. C. Jones, J. T. M. B. Janssen, J. Singleton, and J. A. A. J. Perenboom, "Ballistic transport in one dimension: Additional quantisation produced by an electric field," J. Phys.: Condens. Matter **2**, 7247–7254 (1990).
[22]K. Gloos, P. Utko, M. Aagesen, C. B. Sørensen, J. B. Hansen, and P. E. Lindelof, "Current-voltage characteristics of quantum-point contacts in the closed-channel regime: Transforming the bias voltage into an energy scale," Phys. Rev. B **73**, 125326 (2006).
[23]B. Kaestner, V. Kashcheyevs, G. Hein, K. Pierz, U. Siegner, and H. W. Schumacher, "Robust single-parameter quantized charge pumping," Appl. Phys. Lett. **92**, 192106 (2008).
[24]J. P. Pekola, O.-P. Saira, V. F. Maisi, A. Kemppinen, M. Möttönen, Y. A. Pashkin, and D. V. Averin, "Single-electron current sources: Toward a refined definition of the ampere," Rev. Mod. Phys. **85**, 1421–1472 (2013).